JACS
JOURNAL OF THE AMERICAN CHEMICAL SOCIETY
Communication
pubs.acs.org/JACS

Microwave Synthesis of Microstructured and Nanostructured Metal Chalcogenides from Elemental Precursors in Phosphonium Ionic Liquids

Kunlun Ding, Hong Lu, Yichi Zhang, Matthew L. Snedaker, Deyu Liu, Juan Antonio Maciá-Agulló, and Galen D. Stucky*

Department of Chemistry and Biochemistry, University of California, Santa Barbara, California 93106-9510, United States

Supporting Information

ABSTRACT: We describe a general approach for the synthesis of micro-/nanostructured metal chalcogenides from elemental precursors. The excellent solubility of sulfur, selenium, and tellurium in phosphonium ionic liquids promotes fast reactions between chalcogens and various metal powders upon microwave heating, giving crystalline products. This approach is green, universal, and scalable.

Nanostructured metal chalcogenides are of great importance because of their superior semiconducting properties. In recent years, the demonstrated performance of chalcogenide thermoelectric materials[1−4] ($(Pb,Sb,Bi)_x(Se,Te)_y$ compounds) and topological insulators[5−7] (Bi_2Se_3, Bi_2Te_3, Sb_2Te_3, etc.) has evoked renewed interest in developing protocols for the rational synthesis of metal chalcogenide nanostructures.

Bottom-up chemical synthesis of metal chalcogenides usually starts with metal salts and organochalcogen compounds, as well as certain ligands and solvents. The rather complex chemistries not only generate side products but also limit the yields of the target materials. The difficulty of ligand removal is another limiting factor inhibiting their electronic applications. Nevertheless, extensive effort has been devoted to this field.[8,9] On the other hand, top-down approaches, including ball-milling[10,11] and metallurgy-derived pathways,[3,12,13] have received special emphasis in thermoelectric-material synthesis. Significant breakthroughs have been achieved in the past decade. However, these processes are energy intensive.

Microwave-driven ionothermal synthesis is an alternative approach which, if successful, offers numerous opportunities. Ionic liquids have negligible vapor pressure, high solubilities for many inorganic and organic compounds, strong microwave-absorbing ability, and weak coordination strength. These features of ionic liquids make the ionothermal synthesis an ideal pathway for many inorganic nanomaterials.[14−17] Ionothermal syntheses of metal, metal oxide, and metal chalcogenide nanomaterials have been explored. To date, most of the studies have focused on the use of imidazolium ionic liquids. However, the poor thermal and chemical stabilities of imidazolium ionic liquids greatly limit their applications in inorganic synthesis. Although phosphonium ionic liquids usually have higher thermal and chemical stabilities compared to imidazolium ionic liquids, phosphonium ionic liquids have received much less attention.[18−21]

In this research, we discovered that phosphonium ionic liquids are good solvents for sulfur, selenium, and tellurium at elevated temperatures. The dissolved chalcogens rapidly react with various elemental metal powders upon microwave heating, producing micro-/nanostructured metal chalcogenides. In principle, this type of reaction is the simplest and most straightforward reaction for metal chalcogenide synthesis. It has the highest atom economy. The weak binding strength of the phosphonium ionic liquids enables the nearly complete removal of organic residue via simple washing. Some halogen doping of the chalcogenide product is observed, and the effect of that on the thermoelectric properties of the metal chalcogenides is described.

We first studied the dissolution behavior of sulfur, selenium, and tellurium in tetrabutylphosphonium chloride ($[P_{4\,4\,4\,4}]Cl$), which is a colorless liquid beyond its melting temperature (T_m = 70.6 °C). In our experiments, 4 mmol of sublimed sulfur quickly dissolved in 4 g of $[P_{4\,4\,4\,4}]Cl$ at 105 °C upon magnetic stirring and gave a transparent light yellow solution. The color turned to red in less than an hour, implying the formation of sulfur free-radical chains.[22,23] Later on, it gradually turned to dark brown when aged at 105 °C for 12 h, and the viscosity of the solution was significantly increased, indicating an increase in the chain length of sulfur species.[22,23]

Compared to sulfur, negligible solubility of selenium and tellurium in $[P_{4\,4\,4\,4}]Cl$ was observed at 105 °C. However, after 5 min of microwave heating at 240 °C, 2 mmol of selenium completely dissolved in 4 g of $[P_{4\,4\,4\,4}]Cl$, giving a dark brown solution. During the cooling process, visible needle-shaped selenium microcrystals crystallize from the solution (Figure 1A). This recrystallization process is repeatable in further cycles of microwave heating and cooling. Scanning electron microscopy (SEM) images (Figures 1B,C and S1) show that the irregularly shaped pristine selenium microparticles are completely converted to sub-millimeter-long, 5-μm-wide microrods during the recrystallization process. XRD patterns (Figure S1) suggest that the recrystallized selenium phases have hexagonal crystal lattices that are identical to that of the precursor selenium. However, the (100) and (110) Bragg diffraction peaks become stronger compared to the (101) peak

Received: August 21, 2014
Published: October 21, 2014

   dx.doi.org/10.1021/ja508628q | J. Am. Chem. Soc. 2014, 136, 15465−15468

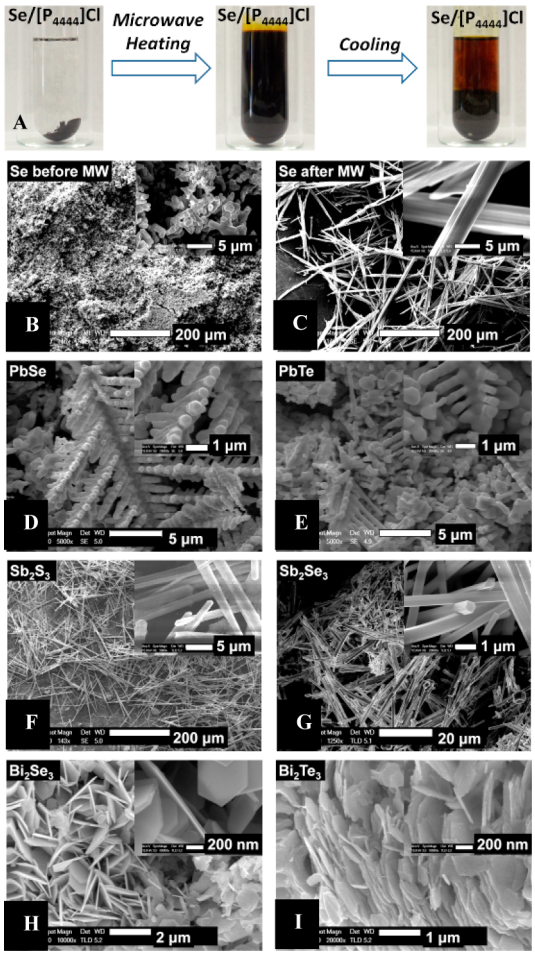

Figure 1. (A) Digital photographs of the Se recrystallization process in $[P_{4\ 4\ 4\ 4}]Cl$. SEM images of Se before (B) and after (C) recrystallization process in $[P_{4\ 4\ 4\ 4}]Cl$, and PbSe (D), PbTe (E), Sb_2S_3 (F), Sb_2Se_3 (G), Bi_2Se_3 (H), and Bi_2Te_3 (I) synthesized from microwave heating of corresponding elemental precursors in $[P_{4\ 4\ 4\ 4}]Cl$.

after recrystallization. This is because of the fact that the selenium microrods are elongated in the [001] direction and prefer lying on the substrate, so that higher percentages of the (100) and (110) planes are parallel to the substrate surface during XRD collection. Similar recrystallization behavior and morphology changes are also observed for tellurium in $[P_{4\ 4\ 4\ 4}]$ Cl ionic liquid upon microwave heating and cooling (Figure S2).

We next studied the reactions between various metals and chalcogens (sulfur, selenium, and tellurium) in order to synthesize metal chalcogenide micro-/nanostructures. Late transition metals were chosen as candidates because of their comparatively lower propensities to form passivating surface layers. We mainly focused on Pb, Sb, and Bi, as their chalcogenides (particularly selenides and tellurides) are of considerable potential importance in thermoelectric-material and topological insulator applications. All the reactions were performed under microwave heating.

Pb and Bi react with Se and Te stoichiometrically at 240 °C under microwave heating. Phase-pure PbSe (cubic, Figure S3), PbTe (cubic, Figure S3), Bi_2Se_3 (rhombohedral, Figure S4), and Bi_2Te_3 (rhombohedral, Figure S4) are formed. SEM images (Figures 1D,E and S5) show that the typical morphologies of the PbSe and PbTe products are highly branched and composed of smaller crystallites with a size of a few hundred nanometers. Bi_2Se_3 and Bi_2Te_3 crystallize in a hexagonal nanoplate shape (Figures 1H,I and S5) with a thickness of 20–50 nm and an edge length of 200 nm to 1 μm. The crystallite sizes of Bi_2Se_3 ([015] direction) and Bi_2Te_3 ([015] direction) are 55 and 49 nm as calculated from the Scherrer equation; these sizes are consistent with the thicknesses of these nanoplates as observed by our SEM observations. Se usually reacts more rapidly than Te. Sb reacts with Se at 240 °C under microwave heating in 20 min and gives phase-pure Sb_2Se_3 microrods (Figures 1G, S5, and S6), while under the same reaction conditions Sb and Te are only partially converted to Sb_2Te_3, even after 30 min (Figure S7).

Sulfur reactions show a quite different behavior than the Se and Te reactions. Sb reacts with sulfur with a Sb/S molar ratio of 1/2, resulting in a transparent solution. Amorphous precipitates form once ethanol is added to the solution. Increasing the Sb/S molar ratio to 2/3 leads to the formation of orthorhombic-phase Sb_2S_3 microrods (Figures 1F, S5, and S6), similar to the Sb_2Se_3 products. Bi reacts with sulfur with a Bi/S molar ratio of 2/3, resulting in a Bi_2S_3 nanobelt structure (Figure S8). Small amorphous particles were observed at lower Bi/S ratios, which might originate from the precipitation of Bi–S species during the washing process.

The detailed reaction mechanism may vary with different metals. Generally speaking, the elemental chalcogens dissolve in phosphonium ionic liquids, which then aggressively react with the metal particles by a corrosive etching mechanism. The retention of the macroscopic morphology and size of the metal precursors confirms the solid-to-solid conversion mechanism (Figures S8 and S9).

In order to test the universality of our synthetic protocol, we extended our study to Cu, In, and Sn. Cu reacts with S, Se, and Te to give $Cu_{2-x}Z$ (Z = S, Se, and Te). SEM images (Figures 2A–C and S10) show that the products are mainly composed

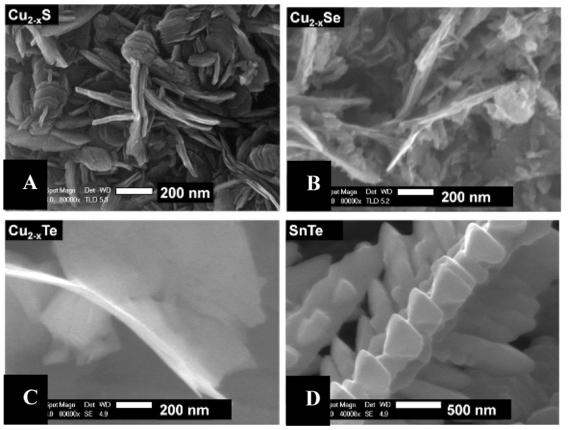

Figure 2. SEM images of (A) $Cu_{2-x}S$, (B) $Cu_{2-x}Se$, (C) $Cu_{2-x}Te$, and (D) SnTe synthesized from microwave heating of corresponding elemental precursors in $[P_{4\ 4\ 4\ 4}]Cl$.

of aggregated nanoplates or nanosheets. XRD patterns of these materials are given in Figures S11 and S12. Similar to the "Sb + S" system, In and Sn react with sulfur (metal/S molar ratio of 1/2) to give transparent solutions, implying the formation of soluble In–S and Sn–S species. Sn and Se with a molar ratio of 1/1 give a transparent solution and unreacted Sn. Compared to sulfur and Se, Te has lower propensity to form soluble species.

dx.doi.org/10.1021/ja508628q | J. Am. Chem. Soc. 2014, 136, 15465–15468

Accordingly, the cubic phase SnTe (Figures 2D and S12) is formed with a morphology similar to that of the PbTe product.

We further tested several different types of phosphonium ionic liquids: tetrabutylphosphonium bromide ([$P_{4\,4\,4\,4}$]Br, T_m = 100−103 °C), tributyl(octyl)phosphonium chloride ([$P_{4\,4\,4\,8}$]Cl, T_m = 19.4 °C), tributyl(tetradecyl)phosphonium chloride ([$P_{4\,4\,4\,14}$]Cl, T_m = 38.9 °C), trihexyl(tetradecyl)-phosphonium chloride ([$P_{6\,6\,6\,14}$]Cl, T_m = −69.8 °C), trihexyl(tetradecyl)phosphonium bromide ([$P_{6\,6\,6\,14}$]Br, T_m = −61 °C), trihexyl(tetradecyl)phosphonium bis-(trifluoromethane)sulfonimide ([$P_{6\,6\,6\,14}$]TFSI, T_m = −72.4 °C). All of these ionic liquids show good solubility of sulfur at 110 °C (>0.5 mmol/g). [$P_{4\,4\,4\,4}$]Br was tested for PbSe and PbTe microwave synthesis. Similar morphologies were obtained compared to that of the [$P_{4\,4\,\ 4\,4}$]Cl-mediated processes (Figure S13). A control experiment on "Pb + Te" reaction in [$P_{4\,4\,4\,4}$]Br employing conventional heating revealed that 30 min is not enough to fully convert all the precursors (Figure S14), implying the advantages of microwave heating in inorganic synthesis.

Another advantage of our synthetic protocol is the negligible vapor pressure of the ionic liquids. Figure 3A shows a typical heating profile of [$P_{4\,4\,4\,4}$]Cl. The pressure of the microwave reactor was close to 1 atm when [$P_{4\,4\,4\,4}$]Cl was heated to 240 °C. During PbTe synthesis in [$P_{4\,4\,4\,4}$]Cl, less than 2 atm of pressure was observed (Figure 3B). Attenuated total reflectance Fourier transform infrared spectroscopy (ATR-FTIR) spectra of the fresh [$P_{4\,4\,4\,4}$]Cl and recovered [$P_{4\,4\,4\,4}$]Cl from PbTe synthesis show no obvious differences (Figure 3C), confirming the excellent thermal and chemical stabilities of the phosphonium ionic liquids. In addition, ATR-FTIR spectra of microwave-synthesized PbSe and PbTe do not show any peak from [$P_{4\,4\,4\,4}$]Cl (Figure 3D), indicating that the ionic liquid was thoroughly removed after washing. Therefore, these ionic liquids have the potential to be reused for subsequent syntheses. In most solution-mediated syntheses of metal chalcogenides, strong-binding molecular bases are used to guide the crystallization of the metal chalcogenides. These bases, for instance, trialkylphosphines and amines, form strong covalent bonds with the chalcogen atoms. This leads to the issue of their post-synthesis removal.[8,9] In our case, the comparatively weak interactions between chalcogens and phosphonium ionic liquids, as demonstrated by the easy recrystallization of the pure chalcogens, allow us to easily remove the ligands after synthesis. This important feature is beneficial for the processing of chalcogenide-based materials for electronic and optical applications.[9] The weak binding is, on the other hand, the reason for the morphology and size of the metal chalcogenide particles obtained in this work. One should bear in mind that the binding strengths of the ligands with the metal chalcogenides surface not only determine the difficulty of post-synthesis ligand removal but also control the particle morphology and dimensions.

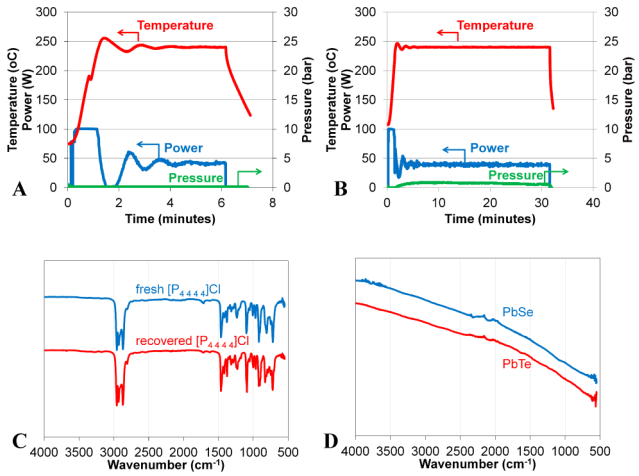

Figure 3. Microwave heating profiles (temperature, power, and pressure) of pure [$P_{4\,4\,4\,4}$]Cl (A) and PbTe synthesis in [$P_{4\,4\,4\,4}$]Cl (B). ATR-FTIR spectra of fresh [$P_{4\,4\,4\,4}$]Cl and recovered [$P_{4\,4\,4\,4}$]Cl from PbTe synthesis (C), and of PbSe and PbTe synthesized from microwave heating of corresponding elemental precursors in [$P_{4\,4\,4\,4}$]Cl (D).

The scalability of our synthetic protocol was also tested. In a single batch run, 10 mmol of Pb and 10 mmol of Se were completely converted in 13.2 g of [$P_{4\,4\,4\,4}$]Cl at 240 °C to 3 g of PbSe in 20 min by heating in a 10−20 mL microwave reactor. The product morphology of this PbSe is identical to that observed for the smaller-scale synthesis. This volumetric productivity is 1−2 orders of magnitude higher than that previously reported for the microwave syntheses of metal chalcogenides.[24,25]

Our preliminary thermoelectric tests show n-type behavior for both the PbSe and PbTe materials synthesized via our method. Compared to the well-studied p-type lead chalcogenide thermoelectric materials, less synthetic and characterization effort has been devoted to their n-type counterparts until recent years.[26,27]

Halogens have been proven to be promising dopants for n-type thermoelectric materials, with most of these halogen-doped materials being generated by solid-state syntheses.[27−30] An efficient solution synthesis has not been developed. We attribute doping by the halogen atoms, which are contained in the phosphonium halide ionic liquids utilized in our solution synthesis, to be the origin of the n-type behavior for the metal chalcogenide products described here. Here the PbTe material synthesized in [$P_{4\,4\,\ 4\,4}$]Br shows a relatively high power factor[28,30] mainly because of its prominent Seebeck coefficient (Figure 4). The electrical conductivity of the PbTe materials obtained in this work is less than that of iodine-doped bulk PbTe materials prepared by more conventional synthetic

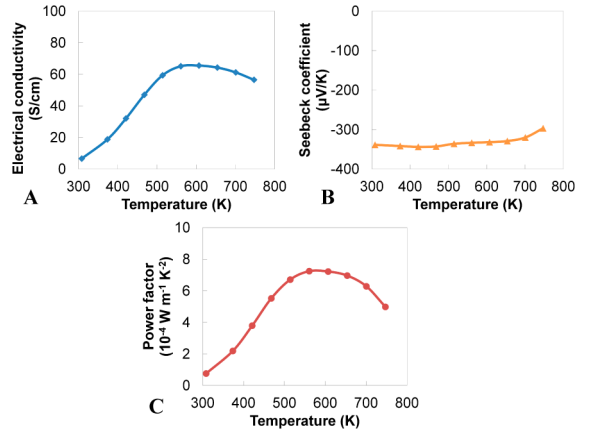

Figure 4. Thermoelectric property measurement of PbTe materials synthesized in [$P_{4\,4\,4\,4}$]Br after spark plasma sintering: temperature dependence of (A) electrical conductivity, (B) Seebeck coefficient, and (C) power factor.

dx.doi.org/10.1021/ja508628q | J. Am. Chem. Soc. 2014, 136, 15465−15468

approaches.[28] Possible reasons are the sub-micrometer-scale crystallite sizes (~500 nm) and lower carrier concentration (as described below) of our PbTe materials. However, compared to the iodine-doped PbTe nanocrytals (<50 nm) previously reported,[30] the electrical conductivity of the PbTe materials in this work is greater by a factor of 100. We believe that the reasons for this difference are the relatively larger nanocrystallite size and easier ligand removal.

Energy-dispersive X-ray (EDX) spectroscopy on a FEI XL40 Sirion scanning electron micrograph was used to analyze the compositions of the materials, as synthesized, after being pressed and after high-temperature measurements, respectively. The halogen concentrations in all the materials were generally below the EDX detection limit (<1%). Nevertheless, the presence of Br in the PbTe materials synthesized in $[P_{4\,4\,4\,4}]Br$ was qualitatively confirmed (Figure S15) by SEM-EDX.

The Van der Pauw method was used to characterize the carrier concentration of the materials. The unintentional n-type doping by the halogens, both Cl and Br, in PbTe gives a carrier concentration of about $4 \times 10^{17}/cm^3$. To achieve an appreciable figure of merit, an optimal doping level is necessary. For the n-type PbTe and PbSe, the optimal halogen doping level is determined to be in the range of $10^{19}-10^{20}/cm^3$.[27,28,31] The doping level obtained in our materials is orders of magnitude lower than the desired optimal value. By optimizing the n-type doping levels in our approach, the thermoelectric performance might be further enhanced.

In summary, we have demonstrated the microwave-assisted ionothermal solution synthesis of metal chalcogenide micro-/nanostructures based on simple chemistry. Various metal chalcogenides were successfully synthesized from their elemental precursors on a relatively large scale. The excellent thermal and chemical stabilities of the phosphonium ionic liquids as well as their high chalcogen solubility make possible a rapid reaction between chalcogens and metal powders at elevated temperatures. Furthermore, the ionic liquids can be easily removed from the products via washing because of the weak-binding feature of the ionic liquids, a feature that is potentially beneficial for many electronic applications, such as thermoelectrics and topological insulators.

■ ASSOCIATED CONTENT

Supporting Information

Experimental details and Figures S1–S15. This material is available free of charge via the Internet at http://pubs.acs.org.

■ AUTHOR INFORMATION

Corresponding Author

stucky@chem.ucsb.edu

Notes

The authors declare no competing financial interest.

■ ACKNOWLEDGMENTS

This research was supported by the Center for Energy Efficient Materials, an Energy Frontier Research Center funded by the U.S. Department of Energy, Office of Science, Basic Energy Sciences under Award No. DE-SC0001009, and by the National Science Foundation (DMR 0805148). We thank Cytec Industries Inc. for kindly providing us several types of phosphonium ionic liquids without cost. The MRL Shared Experimental Facilities are supported by the MRSEC Program of the NSF under Award No. DMR 1121053(a member of the NSF-funded Materials Research Facilities Network, www.mrfn.org).

■ REFERENCES

(1) Dresselhaus, M. S.; Chen, G.; Tang, M. Y.; Yang, R. G.; Lee, H.; Wang, D. Z.; Ren, Z. F.; Fleurial, J. P.; Gogna, P. *Adv. Mater.* **2007**, *19*, 1043.

(2) Minnich, A. J.; Dresselhaus, M. S.; Ren, Z. F.; Chen, G. *Energy Environ. Sci.* **2009**, *2*, 466.

(3) Vineis, C. J.; Shakouri, A.; Majumdar, A.; Kanatzidis, M. G. *Adv. Mater.* **2010**, *22*, 3970.

(4) Pei, Y. Z.; Wang, H.; Snyder, G. J. *Adv. Mater.* **2012**, *24*, 6125.

(5) Zhang, H. J.; Liu, C. X.; Qi, X. L.; Dai, X.; Fang, Z.; Zhang, S. C. *Nat. Phys.* **2009**, *5*, 438.

(6) Moore, J. E. *Nature* **2010**, *464*, 194.

(7) Qi, X. L.; Zhang, S. C. *Rev. Mod. Phys.* **2011**, *83*, 1057.

(8) Malik, M. A.; Afzaal, M.; O'Brien, P. *Chem. Rev.* **2010**, *110*, 4417.

(9) Talapin, D. V.; Lee, J. S.; Kovalenko, M. V.; Shevchenko, E. V. *Chem. Rev.* **2010**, *110*, 389.

(10) Ma, Y.; Hao, Q.; Poudel, B.; Lan, Y. C.; Yu, B.; Wang, D. Z.; Chen, G.; Ren, Z. F. *Nano Lett.* **2008**, *8*, 2580.

(11) Poudel, B.; Hao, Q.; Ma, Y.; Lan, Y. C.; Minnich, A.; Yu, B.; Yan, X. A.; Wang, D. Z.; Muto, A.; Vashaee, D.; Chen, X. Y.; Liu, J. M.; Dresselhaus, M. S.; Chen, G.; Ren, Z. F. *Science* **2008**, *320*, 634.

(12) Pei, Y. Z.; Shi, X. Y.; LaLonde, A.; Wang, H.; Chen, L. D.; Snyder, G. J. *Nature* **2011**, *473*, 66.

(13) Biswas, K.; He, J. Q.; Blum, I. D.; Wu, C. I.; Hogan, T. P.; Seidman, D. N.; Dravid, V. P.; Kanatzidis, M. G. *Nature* **2012**, *489*, 414.

(14) Antonietti, M.; Kuang, D. B.; Smarsly, B.; Yong, Z. *Angew. Chem., Int. Ed.* **2004**, *43*, 4988.

(15) Plechkova, N. V.; Seddon, K. R. *Chem. Soc. Rev.* **2008**, *37*, 123.

(16) Ma, Z.; Yu, J. H.; Dai, S. *Adv. Mater.* **2010**, *22*, 261.

(17) Freudenmann, D.; Wolf, S.; Wolff, M.; Feldmann, C. *Angew. Chem., Int. Ed.* **2011**, *50*, 11050.

(18) Bradaric, C. J.; Downard, A.; Kennedy, C.; Robertson, A. J.; Zhou, Y. H. *Green Chem.* **2003**, *5*, 143.

(19) Sowmiah, S.; Srinivasadesikan, V.; Tseng, M. C.; Chu, Y. H. *Molecules* **2009**, *14*, 3780.

(20) Adamova, G.; Gardas, R. L.; Rebelo, L. P. N.; Robertson, A. J.; Seddon, K. R. *Dalton Trans.* **2011**, *40*, 12750.

(21) Adamova, G.; Gardas, R. L.; Nieuwenhuyzen, M.; Puga, A. V.; Rebelo, L. P. N.; Robertson, A. J.; Seddon, K. R. *Dalton Trans.* **2012**, *41*, 8316.

(22) Meyer, B. *Chem. Rev.* **1976**, *76*, 367.

(23) Chung, W. J.; Griebel, J. J.; Kim, E. T.; Yoon, H.; Simmonds, A. G.; Ji, H. J.; Dirlam, P. T.; Glass, R. S.; Wie, J. J.; Nguyen, N. A.; Guralnick, B. W.; Park, J.; Somogyi, A.; Theato, P.; Mackay, M. E.; Sung, Y. E.; Char, K.; Pyun, J. *Nat. Chem.* **2013**, *5*, 518.

(24) Dong, G. H.; Zhu, Y. J.; Chen, L. D. *J. Mater. Chem.* **2010**, *20*, 1976.

(25) Mehta, R. J.; Zhang, Y. L.; Karthik, C.; Singh, B.; Siegel, R. W.; Borca-Tasciuc, T.; Ramanath, G. *Nat. Mater.* **2012**, *11*, 233.

(26) Snyder, G. J.; Toberer, E. S. *Nat. Mater.* **2008**, *7*, 105.

(27) Wang, H.; Pei, Y. Z.; LaLonde, A. D.; Snyder, G. J. *Proc. Natl. Acad. Sci. U.S.A.* **2012**, *109*, 9705.

(28) (a) LaLonde, A. D.; Pei, Y. Z.; Snyder, G. J. *Energy Environ. Sci.* **2011**, *4*, 2090. (b) Nikolic, M. V.; Paraskevopoulos, K. M.; Hatzikraniotis, E.; Nikolic, N.; Vujatovic, S. S.; Aleksic, O. S.; Zorba, T. T.; Kyratsi, Th.; Menicanin, A.; Nikolic, P. M. *AIP Conf. Proc. (ICT2011)* **2012**, *1449*, 143.

(29) Rhyee, J. S.; Ahn, K.; Lee, K. H.; Ji, H. S.; Shim, J. H. *Adv. Mater.* **2011**, *23*, 2191.

(30) Fang, H. Y.; Luo, Z. Q.; Yang, H. R.; Wu, Y. *Nano Lett.* **2014**, *14*, 1153.

(31) Parker, D.; Singh, D. J.; Zhang, Q. Y.; Ren, Z. F. *J. Appl. Phys.* **2012**, *111*, 123701.